Inorg. Chem. **2004**, *43*, 1481–1490

Syntheses, Structures, and Redox Properties of Dimeric Triruthenium Clusters Bridged by Bis(diphenylphosphino)acetylene and -ethylene

Jing-Lin Chen,[†] Li-Yi Zhang,[†] Zhong-Ning Chen,*[,†,‡] Li-Bin Gao,[†] Masaaki Abe,[§] and Yoichi Sasaki[§]

State Key Laboratory of Structural Chemistry, Fujian Institute of Research on the Structure of Matter and Graduate School of the Chinese Academy of Sciences, Fuzhou, Fujian 350002, China, State Key Laboratory of Coordination Chemistry, Nanjing University, Nanjing 210093, China, and Division of Chemistry, Graduate School of Science, Hokkaido University, Sapporo 060-0810, Japan

Received May 11, 2003

Reactions of oxo-centered triruthenium acetate complexes $[Ru_3O(OAc)_6(py)_2(CH_3OH)](PF_6)$ (py = pyridine, OAc = CH_3COO^-) (**1**) with nearly equimolar amounts of dppa {bis(diphenylphosphino)acetylene} or dppen {*trans*-1,2-bis(diphenylphosphino)ethylene} gave $[Ru_3O(OAc)_6(py)_2(L)](PF_6)$ (L = dppa, **2**; dppen, **3**). With 2.4 equiv of **1**, the reactions provided diphosphine-linked triruthenium dimers, $[\{Ru_3O(OAc)_6(py)_2\}_2(L)](PF_6)_2$ (L = dppa, **4**; L = dppen, **5**), respectively. Similarly, the reactions of $[Ru_3O(OAc)_6(L')_2(MeOH)]^+$ {L′ = dmap (4-(dimethylamino)pyridine), **1a**; L′ = abco (1-azabicyclo[2.2.2]octane), **1b**} with dppen gave dppen-linked dimers, $[\{Ru_3O(OAc)_6(dmap)_2\}_2(dppen)](SbF_6)_2$ (**6**) and $[\{Ru_3O(OAc)_6(abco)_2\}_2(dppen)](BF_4)_2$ (**7**), respectively. The chemical reduction of **2**, **4**, and **5** by hydrazine afforded one- or two-electron-reduced, neutral products, $Ru_3O(OAc)_6(py)_2(dppa)$ (**2a**), $\{Ru_3O(OAc)_6(py)_2\}_2(dppa)$ (**4a**), and $\{Ru_3O(OAc)_6(py)_2\}_2(dppen)$ (**5a**), respectively. The complexes were characterized by elemental analyses, ES-MS, UV–vis, IR, and ^{31}P NMR spectroscopies, and cyclic and differential-pulse voltammetries. The molecular structures of compounds **2**, **4**, **5**, **5a**, **6**, and **7** were determined by single-crystal X-ray diffraction. In 0.1 M $(Bu_4N)PF_6$–acetone, the monomers and dimers of triruthenium clusters show reversible and multistep redox responses. The two triruthenium cluster centers in dimers undergo stepwise reductions and oxidations due to the identical redox processes of the individual Ru_3O cluster cores, suggesting the presence of electronic communications between them through the conjugated diphosphine spacer. The redox wave splitting mediated by dppa containing an ethynyl group (C≡C) is found to be more extensive than that by dppen containing an ethenyl (C═C) one. It appears that the redox wave splitting is enhanced by the introduction of electron-donating substituents on the auxiliary pyridine rings.

Introduction

Multinuclear transition metal complexes that exhibit ligand-mediated metal-to-metal electronic communications, including electron-/energy-transfer phenomena, are extensively investigated because of their potential application to molecular-scale electronics and devices.[1,2] Recent interest in such functional complexes has intensified due to their potential use in the development of materials with properties such as conductivity, photo-/electroluminescence, magnetism, and nonlinear optics.[1,3] Furthermore, these complexes are attractive as they can provide intriguing mixed-valence species that are regarded as prototypes for molecular switches and wires.

A key to good multicentered metal-based material is the choice of bridging ligands capable of mediating electronic

* Corresponding author. Fax: +86-591-379-2346. E-mail: czn@ms.fjirsm.ac.cn.
[†] Fujian Institute of Research on the Structure of Matter.
[‡] Nanjing University.
[§] Hokkaido University.

(1) (a) Demadis, K. D.; Hartshorn, C. M.; Meyer, T. J. *Chem. Rev.* **2001**, *101*, 2655−2686. (b) Paul, F.; Lapinte, C. *Coord. Chem. Rev.* **1998**, *178*−*180*, 431−509. (c) Ziessel, R.; Hissler, M.; El-ghayoury, A.; Harriman, A. *Coord. Chem. Rev.* **1998**, *178*−*180*, 1251−1298. (d) Cotton, F. A.; Lin, C.; Murillo, C. A. *Acc. Chem. Res.* **2001**, *34*, 759−771. (e) Barigelletti, F.; Flamigni, L. *Chem. Soc. Rev.* **2000**, *29*, 1−12. (f) Astruc, D. *Acc. Chem. Res.* **1997**, *30*, 383−391. (g) Kaim, W.; Klein, A.; Glöckle, M. *Acc. Chem. Res.* **2000**, *33*, 755−763. (h) Carroll, R. L.; Gorman, C. B. *Angew. Chem., Int. Ed.* **2002**, *41*, 4378−4400.

(2) (a) Creutz, C. Taube, H. *J. Am. Chem. Soc.* **1973**, *95*, 1086−1094. (b) Richardson, D. E.; Taube, H. *Coord. Chem. Rev.* **1984**, *60*, 107−129. (c) Callahan, R. W.; Keene, F. R.; Meyer, T. J.; Salmon, D. J. *J. Am. Chem. Soc.* **1977**, *99*, 1064−1073.

10.1021/ic0344968 CCC: $27.50
Published on Web 01/16/2004

communications. The spacers used so far are in most cases either conjugated N-/O-donor or often C-donor ligands connected by sp or sp^2 carbon chains.[3−10] Conjugated diphosphines with sp or sp^2 carbon chains between the two phosphorus donors[11−13] have been ignored in some sense, however. Like the conjugated C- or N-donor ligands, the rodlike P-donor spacers also exhibit some characteristics such as rigidity, conjugation, and photostability, as well as having molecular orbitals with suitable energies to overlap with those of the attached metal centers. Thus, by using tunable rigid spacers between two P donors, the distances and the extent of the communications between metal centers are controllable.

A proper choice of metal centers is another important point for attaining good electronic communications between them. Compared with relatively abundant examples of mononuclear redox-active building blocks,[1−3,7−9,11] much fewer polynuclear cluster moieties are known for the design of molecular wires.[4−6,10] The oxo-centered triruthenium carboxylate clusters with general formula $[Ru_3(\mu_3\text{-}O)(\mu\text{-}O_2CR)_6L_3]^n$ (R = alky or aryl, L = axial ligands) are promising building blocks as they exhibit multiple redox behavior, rich mixed-valence chemistry, and catalytic properties.[14−17] The richness of the triruthenium chemistry is enhanced by the diverse substitution chemistry of the axial ligands L. Thus, a variety of combination of mixed terminal ligands has been achieved. This makes possible not only affording a means to design dimeric and oligomeric triruthenium clusters by using proper bridging ligands,[5,6,16] but also tuning the electronic state of the triruthenium center. Solvent-coordinated triruthenium compounds such as $[Ru_3(\mu_3\text{-}O)(\mu\text{-}O_2CR)_6L_2(S)]^-$, $Ru_3(\mu_3\text{-}O)(\mu\text{-}O_2CR)_6(CO)L(S)$, and $Ru_3(\mu_3\text{-}O)(\mu\text{-}O_2CR)_6(CO)(S)_2$ (S = solvent molecules such as H_2O and CH_3OH) are the most useful precursors for the design of ligand-linked oligomeric molecular materials based on $Ru_3(\mu_3\text{-}O)(\mu\text{-}O_2CR)_6$ cores.[6b,14c] Dimers, trimers, and hexamers of triruthenium clusters bridged by pyrazine and 4,4′-bipyridine have been reported which exhibit extensive

(3) (a) Hoshino, Y.; Higuchi, S.; Fiedler, J.; Su, C.-Y.; Knodler, A.; Schwederski, B.; Sarkar, B.; Hartmann, H.; Kaim, W. *Angew. Chem., Int. Ed*. **2003**, *42*, 674−677. (b) Patoux, C.; Launay, J.-P.; Beley, M.; Chodorowski-Kimmes, S.; Collin, J.-P.; James, S.; Sauvage, J.-P. *J. Am. Chem. Soc*. **1998**, *120*, 3717−3725. (c) Laye, R. H.; Couchman, S. M.; Ward, M. D. *Inorg. Chem*. **2001**, *40*, 4089−4092. (d) Mosher, P. J.; Yap, G. P. A.; Crutchley, R. J. *Inorg. Chem*. **2001**, *40*, 1189−1195. (e) Cameron, C. C.; Pickup, P. G. *J. Am. Chem. Soc*. **1999**, *121*, 7710−7711.

(4) (a) Londergan, C. H.; Salsman, J. C.; Ronco, S.; Dolkas, L. M.; Kubiak, C. P. *J. Am. Chem. Soc*. **2002**, *124*, 6236−6237. (b) Londergan, C. H.; Salsman, J. C.; Ronco, S.; Kubiak, C. P. *Inorg. Chem*. **2003**, *42*, 926−928. (c) Zavarine, I. S.; Kubiak, C. P.; Yamaguchi, T.; Ota, K.; Matsui, T.; Ito, T. *Inorg. Chem*. **2000**, *39*, 2696−2698.

(5) (a) Ito, T.; Hamaguchi, T.; Nagino, H.; Yamaguchi, T.; Kido, H.; Zavarine, I. S.; Richmond, T.; Washington, J.; Kubiak, C. P. *J. Am. Chem. Soc*. **1999**, *121*, 4625−4632. (b) Ito, T.; Hamaguchi, T.; Nagino, H.; Yamaguchi, T.; Washington, J.; Kubiak, C. P. *Science* **1997**, *277*, 660−663. (c) Ota, K.; Sasaki, H.; Matsui, T.; Hamaguchi, T.; Yamaguchi, T.; Ito, T.; Kido, H.; Kubiak, C. P. *Inorg. Chem*. **1999**, *38*, 4070−4078. (d) Yamaguchi, T.; Imai, N.; Ito, T.; Kubiak, C. P. *Bull. Chem. Soc. Jpn*. **2000**, *73*, 1205−1212. (e) Kido, H.; Nagino, H.; Ito, T. *Chem. Lett*. **1996**, 745−746. (f) Nikolaou, S.; Toma, H. E. *Polyhedron* **2001**, *20*, 253−259.

(6) (a) Baumann, J. A.; Salmon, D. J.; Wilson, S. T.; Meyer, T. J. *Inorg. Chem*. **1979**, *18*, 2472−2479. (b) Baumann, J. A.; Wilson, S. T.; Salmon, D. J.; Hood, P. L.; Meyer, T. J. *J. Am. Chem. Soc*. **1979**, *101*, 2916−2920. (c) Wilson, S. T.; Bondurant, R. F.; Meyer, T. J.; Salmon, D. J. *J. Am. Chem. Soc*. **1975**, *97*, 2285−2287.

(7) (a) Dembinski, R.; Bartik, T.; Bartik, B.; Jaeger, M.; Gladysz, J. A. *J. Am. Chem. Soc*. **2000**, *122*, 810−822. (b) Paul, F.; Meyer, W. E.; Toupet, L.; Jiao, H.; Gladysz, J. A.; Lapinte, C. *J. Am. Chem. Soc*. **2000**, *122*, 9405. (c) Brady, M.; Weng, W.; Zhou, Y.; Seyler, J. W.; Amoroso, A. J.; Arif, A. M.; Böhme, M.; Frenking, G.; Gladysz, J. A. *J. Am. Chem. Soc*. **1997**, *119*, 775−788.

(8) (a) Bruce, M. I.; Low, P. J.; Costuas, K.; Halet, J.-F.; Best, S. P.; Heath, G. A. *J. Am. Chem. Soc*. **2000**, *122*, 1949−1962. (b) Kheradmandan, S.; Heinze, K.; Schmalle, H. W.; Berke, H. *Angew. Chem., Int. Ed.* **1999**, *38*, 2270−2273.

(9) (a) Jones, N. D.; Wolf, M. O.; Giaquinta, D. M. *Organometallics* **1997**, *16*, 1352−1354. (b) Zhu, Y.; Clot, O.; Wolf, M. O.; Yap, G. P. A. *J. Am. Chem. Soc*. **1998**, *120*, 1812−1821. (c) Sato, M.; Hayashi, Y.; Kumakura, S.; Shimizu, N.; Katada, M.; Kawata, S. *Organometallics* **1996**, *15*, 721−728. (d) Lavastre, O.; Plass, J.; Bachmann, P.; Guesmi, S.; Moinet, C.; Dixneuf, P. H. *Organometallics* **1997**, *16*, 184−189. (e) Colbert, M. C. B.; Lewis, J.; Long, N. J.; Raithby, P. R.; White, A. J. P.; Williams, D. J. *J. Chem. Soc., Dalton Trans*. **1997**, 99−104.

(10) (a) Xu, G.-L.; Zou, G.; Ni, Y.-H.; DeRosa, M. C.; Crutchley, R. J.; Ren, T. *J. Am. Chem. Soc*. **2003**, *125*, 10057−10065. (b) Ren, T.; Zou, G.; Alvarez, J. C. *Chem. Commun*. **2000**, 1197−1198. (c) Wong, K.-T.; Lehn, J.-M.; Peng, S.-M.; Lee, G.-H. *Chem. Commun*. **2000**, 2259. (d) Bear, J. L.; Han, B.; Wu, Z.; Van Caemelbecke, E.; Kadish, K. M. *Inorg. Chem*. **2001**, *40*, 2275−2281. (e) Cotton, F. A.; Donahue, J. P.; Murillo, C. A. *J. Am. Chem. Soc*. **2003**, *125*, 5436−5450.

(11) (a) Sullivan, B. P.; Meyer, T. J. *Inorg. Chem*. **1980**, *19*, 752. (b) Xu, D.; Khin, K. T.; van der Veer, W. E.; Ziller, J. W.; Hong, B. *Chem. Eur. J*. **2001**, *7*, 2425−2434. (c) Xu, D.; Hong, B. *Angew. Chem., Int. Ed*. **2000**, *39*, 1826−1829. (d) Hong, B.; Ortega, J. V. *Angew. Chem., Int. Ed*. **1998**, *37*, 2131−2134. (e) Ortega, J. V.; Khin, K.; van der Veer, W. E.; Ziller, J.; Hong, B. *Inorg. Chem*. **2000**, *39*, 6038−6050. (f) Xu, D.; Zhang, J. Z.; Hong, B. *J. Phys. Chem. A* **2001**, *105*, 7979−7988. (g) Ortega, J. V.; Hong, B.; Ghosal, S.; Hemminger, J. C.; Breedlove, B.; Kubiak, C. P. *Inorg. Chem*. **1999**, *38*, 5102−5112. (h) Hong, B.; Woodcock, S. R.; Saito, S. K.; Ortega, J. V. *J. Chem. Soc., Dalton Trans*. **1998**, 2615−2623.

(12) (a) Haid, R.; Gutmann, R.; Stampfl, T.; Langes, C.; Czermak, G.; Kopacka, H.; Ongania, K.-H.; Brggeller, P. *Inorg. Chem*. **2001**, *40*, 7099. (b) Orama, O. *J. Organomet. Chem*. **1986**, *314*, 273−279. (c) Amoroso, A. J.; Johnson, B. F. G.; Lewis, J.; Massey, A. D.; Raithby, P. R.; Wong, W. T. *J. Organomet. Chem*. **1992**, *440*, 219−231. (d) Bruce, M. I.; Humphrey, P. A.; Skelton, B. W.; White, A. H. *Aust. J. Chem.* **1997**, *50*, 535. (e) Adams, C. J.; Bruce, M. I.; Horn, E.; Skelton, B. W.; Tiekink, E. R.; White, A. H. *J. Chem. Soc., Dalton Trans*. **1993**, 3313. (f) Hogarth, G.; Norman, T. *Polyhedron* **1996**, *15*, 2859. (g) Hogarth, G.; Norman, T. *J. Chem. Soc., Dalton Trans*. **1996**, 1077. (h) Louattani, E.; Suades, J.; Urtiaga, K.; Arriortua, M. I.; Solans, X. *Organometallics* **1996**, *15*, 468.

(13) (a) Heinemann, F. W.; Kummer, S.; Seiss-Brandl, U.; Zenneck, U. *Organometallics* **1999**, *18*, 2021. (b) Maitra, K.; Catalano, V. J.; Nelson, J. H. *J. Organomet. Chem*. **1997**, *529*, 409−422. (c) Huy, N. H. T.; Ricard, L.; Mathey, F. *Angew. Chem., Int. Ed*. **2001**, *40*, 1253. (d) Ang, H. G.; Ang, S. G.; Wang, X. *J. Chem. Soc., Dalton Trans*. **2000**, 3429.

(14) (a) Cotton, F. A.; Junior, J. G. N. *Inorg. Chim. Acta* **1972**, *6*, 411−419. (b) Spencer, A.; Wilkinson, G. *J. Chem. Soc., Dalton Trans*. **1974**, 786−793. (c) Baumann, J. A.; Salmon, D. J.; Wilson, S. T.; Meyer, T. J.; Hatfield, W. E. *Inorg. Chem*. **1978**, *17*, 3342−3350.

(15) (a) Sasaki, Y.; Umakoshi, K.; Imamura, T.; Kikuchi, A.; Kishimoto, A. *Pure Appl. Chem*. **1997**, *69*, 205−210. (b) Abe, M.; Sasaki, Y.; Yamada, Y.; Tsukahara, K.; Yano, S.; Yamaguchi, T.; Tominage, M.; Taniguchi, I.; Ito, T. *Inorg. Chem.* **1996**, *35*, 6724−6734. (c) Abe, M.; Sasaki, Y.; Yamada, Y.; Tsukahara, K.; Yano, S.; Ito, T. *Inorg. Chem*. **1995**, *34*, 4490−4498. (d) Abe, M.; Sasaki, Y.; Yamaguchi, T.; Ito, T. *Bull. Chem. Soc. Jpn*. **1992**, *65*, 1585−1590. (e) Abe, M.; Sato, A.; Inomata, T.; Kondo, T.; Uosaki, K.; Sasaki, Y. *J. Chem. Soc., Dalton Trans*. **2000**, 2693−2702. (f) Sasaki, Y.; Tokiwa, A.; Ito, T. *J. Am. Chem. Soc.* **1987**, *109*, 6341−6347.

(16) (a) Toma, H. E.; Araki, K.; Alexiou, A. D. P.; Nikolaou, S.; Dovidauskas, S. *Coord. Chem. Rev.* **2001**, *219*, 187−234. (b) Dovidauskas, S.; Toma, H. E.; Araki, K.; Sacco, H. C.; Iamamoto, Y. *Inorg. Chim. Acta* **2000**, *305*, 206−213. (c) Toma, H. E.; Alexiou, A. D. P.; Dovidauskas, S. *Eur. J. Inorg. Chem*. **2002**, 3010−3017.

(17) (a) Powell, G.; Richens, D. T.; Powell, A. K. *Inorg. Chim. Acta* **1993**, *213*, 147−155. (b) Almog, O.; Bino, A.; Garfinkel-Shweky, D. *Inorg. Chim. Acta* **1993**, *213*, 99−102. (c) Marr, S. B.; Carvel, R. O.; Richens, D. T.; Lee, H.-J.; Lane, M.; Stavropoulos, P. *Inorg. Chem.* **2000**, *39*, 4630−4638.

electronic communications between the triruthenium units.[4−6,16a] The sequential connection of the triruthenium centers performed on a gold electrode surface may be regarded as an approach to the construction of molecular wire on a solid surface. The pentameric triruthenium wire thus prepared by using 4,4′-bipyridine as bridges appears to mediate electronic communications between the cluster units.[18]

For the purpose of designing electronically delocalized molecular wires based on triruthenium clusters, we have been devoted to the construction of dimers of triruthenium clusters linked by conjugated rigid diphosphine spacers. The precursors used for this purpose are $[Ru_3(O)(OAC)_6L_2(MeOH)]^+$ (L = py, [**1**]$^+$; dmap, [**1a**]$^+$; abco, [**1b**]$^+$). The degree of electronic communications between the two triruthenium moieties would be tuned by the choice of both the terminal ligands and the diphosphine spacers. In this paper, we describe the preparation, structural and spectroscopic characterization, and redox properties of the triruthenium cluster dimers connected by conjugated diphosphines.

Experimental Section

General Material. All operations were performed in an atmosphere of dry argon by using Schlenk and vacuum-line techniques. Solvents were dried by standard methods and distilled prior to use. Bis(diphenylphosphino)acetylene (dppa), *trans*-1,2-bis(diphenylphosphino)ethylene (dppen), 4-(dimethylamino)pyridine (dmap), and 1-azabicyclo[2.2.2]octane (abco) were commercially available (Acros, Fluka, or Strem Chemicals Corp.). The precursor compounds $[Ru_3O(OAc)_6(py)_2(CH_3OH)](PF_6)$ (**1**) and $Ru_3O(OAc)_6(CO)(CH_3OH)_2$ were prepared according to reported procedures.[6a,b] $[Ru_3O(OAc)_6(dmap)_2(CH_3OH)](SbF_6)$ (**1a**) and $[Ru_3O(OAc)_6(abco)_2(CH_3OH)](BF_4)$ (**1b**) were synthesized according to the modified procedures described in the literature.[19]

$[Ru_3O(OAc)_6(py)_2(dppa)](PF_6)$ (2). To a CH_2Cl_2 (50 mL) solution of **1** (300 mg, 0.297 mmol) was added dppa (130 mg, 0.330 mmol), and the solution was stirred for 2 days. The solvent was evaporated under vacuum to remain about 3 mL of the green solution which was purified by silica gel column chromatography using $CH_2Cl_2-CH_3OH$ (v/v 50:1) as an eluent to give 365 mg of the product. Yield: 89%. Anal. Calcd for $C_{48}H_{48}F_6N_2O_{13}P_3Ru_3$: C, 42.05; H, 3.53; N, 2.04. Found: C, 41.88; H, 3.19; N, 2.04. ES-MS (*m*/*z*): 1228 $[M - PF_6]^+$, 1243 $[Ru_3O(OAc)_6(py)_2(dppa)(H_2O)]^+$, 1070 $[Ru_3O(OAc)_6(dppa)]^+$. IR spectrum (KBr, cm^{-1}): 2108w (C≡C), 1554m (COO), 1421s (COO), 841s (PF_6). UV−vis spectrum (CH_3CN): λ_{max}/nm (ϵ/dm^3 mol^{-1} cm^{-1}) = 232 (50 040), 404 (5500), 614 (4639), 687 (4350). ^{31}P NMR spectrum (CD_3CN): δ 15.0 (s, Ru−PC≡C*P*), −41.0 (s, Ru−*P*C≡CP), −142.5 (h, $J_{^{31}P-^{19}F}$ = 702 Hz, *P*F_6).

$[Ru_3O(OAc)_6(py)_2(dppa)]$ (2a). To a $CH_2Cl_2-CH_3OH$ (v/v 1:15, 15 mL) solution containing **2** (198 mg, 0.144 mmol) was added dropwise an aqueous solution of hydrazine (ca. 50%), producing a green precipitate. After stirring for 30 min, the precipitate was collected by suction filtration, washed with water, and dried in vacuo. The product was recrystallized from CH_2Cl_2−petroleum ether. Yield: 100 mg, 56%. Anal. Calcd for $C_{48}H_{48}N_2O_{13}P_2Ru_3$: C, 47.02; H, 3.95; N, 2.28. Found: C, 46.63; H, 3.53; N, 2.26. IR spectrum (KBr, cm^{-1}): 2112w (C≡C), 1564m (COO), 1416s (COO). UV−vis spectrum (CH_3CN): λ_{max}/nm (ϵ/dm^3 mol^{-1} cm^{-1}) = 227 (46 720), 385 (8560), 693 (3310), 902 (5470). ^{31}P NMR spectrum (CD_3CN): δ 9.1 (s, Ru−PC≡C*P*), −31.5 (s, Ru−*P*C≡CP).

$[Ru_3O(OAc)_6(py)_2(dppen)](PF_6)$ (3). Complex **3** was synthesized by the method identical to that for **2** except that dppen was used in place of dppa. Yield: 76%. Anal. Calcd for $C_{48}H_{50}F_6N_2O_{13}P_3Ru_3$: C, 41.99; H, 3.67; N, 2.04. Found: C, 41.86; H, 3.21; N, 2.01. ES-MS (*m*/*z*): 1230 $[M - PF_6]^+$, 1152 $[Ru_3O(OAc)_6(py)(dppen)]^+$, 1071 $[Ru_3O(OAc)_6(dppen)]^+$. IR spectrum (KBr, cm^{-1}): 1554m (COO), 1431s (COO), 841s (PF_6). UV−vis spectrum (CH_3CN): λ_{max}/nm (ϵ/dm^3 mol^{-1} cm^{-1}) = 228 (50 740), 399 (5640), 612 (4870), 684 (4850).

$[\{Ru_3O(OAc)_6(py)_2\}_2(dppa)](PF_6)_2$ (4). To a CH_2Cl_2 (45 mL) solution of **1** (240 mg, 0.238 mmol) was added dppa (40 mg, 0.101 mmol) with stirring for 2 days. The green residue obtained by removing the solvent in vacuo was purified by column chromatography (alumina, CH_2Cl_2/CH_3OH,100:1 v/v). Yield: 202 mg, 85%. Anal. Calcd for $C_{70}H_{76}F_{12}N_4O_{26}P_4Ru_6$: C, 35.81; H, 3.26; N, 2.39. Found: C, 35.63; H, 2.96; N, 2.29. ES-MS (*m*/*z*): 1030 $[M - 2PF_6]^{2+}$, 1227 $[Ru_3O(OAc)_6(py)_2(dppa)]^+$, 1051 $[Ru_3O(OAc)_6(py)(dppa)]^+$, 847 $[Ru_3O(OAc)_6(py)_2(H_2O)]^+$. IR spectrum (KBr, cm^{-1}): 2135vw (C≡C), 1556m (COO), 1417s (COO), 841s (PF_6). UV−vis spectrum (MeCN): λ_{max}/nm (ϵ/dm^3 mol^{-1} cm^{-1}) = 235 (78 270), 399 (12 170), 621 (9975), 670 (9765). ^{31}P NMR spectrum (CD_3CN): δ −41.0 (s, Ru−*P*C≡CP−Ru), −142.3 (h, $J_{^{31}P-^{19}F}$ = 708 Hz, *P*F_6).

$\{Ru_3O(OAc)_6(py)_2\}_2(dppa)$ (4a). Complex **4a** was prepared by the same synthetic procedure as that for **2a** except that complex **4** (250 mg, 0.106 mmol) was used in place of **2**. Yield: 175 mg, 80%. Anal. Calcd for $C_{70}H_{76}N_4O_{26}P_2Ru_6$: C, 40.86; H, 3.72; N, 2.72. Found: C, 40.96; H, 3.48; N, 2.67. IR spectrum (KBr, cm^{-1}): 2117w (C≡C), 1566m (COO), 1417s (COO). UV−vis spectrum (MeCN): λ_{max}/nm (ϵ/dm^3 mol^{-1} cm^{-1}) = 231 (45 430), 373 (17 150), 697 (10 740), 914 (14 210). ^{31}P NMR spectrum (CD_3CN): δ −32.2 (s, Ru−*P*C≡CP−Ru).

$[\{Ru_3O(OAc)_6(py)_2\}_2(dppen)](PF_6)_2$ (5). Complex **5** was synthesized by the procedure identical to that for **4** except that dppen was used in place of dppa. Yield: 88%. Anal. Calcd for $C_{70}H_{78}F_{12}N_4O_{26}P_4Ru_6$: C, 35.78; H, 3.35; N, 2.38. Found: C, 35.30; H, 2.99; N, 2.13. ES-MS (*m*/*z*): 1031 $[M - 2PF_6]^{2+}$, 1228 $[Ru_3O(OAc)_6(py)_2(dppen)]^+$, 1147 $[Ru_3O(OAc)_6(py)(dppen)]^+$, 863 $[Ru_3O(OAc)_6(py)_2(CH_3OH)]^+$, 818 $[Ru_3O(OAc)_6(py)(CH_3OH)_2]^+$. IR spectrum (KBr, cm^{-1}): 1556m (COO), 1417s (COO), 843s (PF_6). UV−vis spectrum (CH_3CN): λ_{max}/nm (ϵ/dm^3 mol^{-1} cm^{-1}) = 227 (75 470), 403 (11 190), 620 (9470), 680 (9370). ^{31}P NMR spectrum (CD_3CN): δ 17.5 (s, Ru−*P*CH=CHP−Ru), −142.6 (h, $J_{^{31}P-^{19}F}$ = 708 Hz, *P*F_6).

$[Ru_3O(OAc)_6(py)_2]_2(dppen)$ (5a). To a $CH_2Cl_2-CH_3OH$ (1:5 v/v, 12 mL) solution of **5** (100 mg, 0.042 mmol) was added dropwise an aqueous solution of dilute hydrazine (50%) to produce a precipitate which was collected by suction filtration, washed with water, and dried in vacuo. The residue was recrystallized by layering petroleum ether onto the CH_2Cl_2 solution. Yield: 66 mg, 76%. Anal. Calcd for $C_{70}H_{78}N_4O_{26}P_2Ru_6$: C, 40.70; H, 3.81; N, 2.71. Found: C, 40.42; H, 3.55; N, 2.43. ES-MS: *m*/*z* 1229 $[Ru_3O(OAc)_6(py)_2(dppen)]^+$, 865 $[Ru_3O(OAc)_6(py)_2(CH_3OH)]^+$. IR spectrum (KBr, cm^{-1}): 1562m (COO), 1416s (COO). UV−vis spectrum (CH_3CN): λ_{max}/nm (ϵ/dm^3 mol^{-1} cm^{-1}) = 230 (62 950), 375 (20 420),

(18) Abe, M.; Michi, T.; Sato, A.; Kondo, T.; Zhou, W.; Ye, S.; Uosaki, K.; Sasaki, Y. *Angew. Chem., Int. Ed.* **2003**, *42*, 2912−2915.
(19) Abe, M.; Kondo, T.; Uosaki, K.; Sasaki, Y. *J. Electroanal. Chem.* **1999**, *473*, 93−98.
(20) Sheldrick, G. M. *SHELXL-97, Program for the Refinement of Crystal Structures*; University of Göttingen: Göttingen, Germany, 1997.
(21) Richardson, D. E.; Taube, H. *Inorg. Chem.* **1981**, *20*, 1278−1285.

Scheme 1. Synthetic Pathway for Oxo-Centered Triruthenium Acetate Cluster Based Monomers and Dimers with dppa Ligand

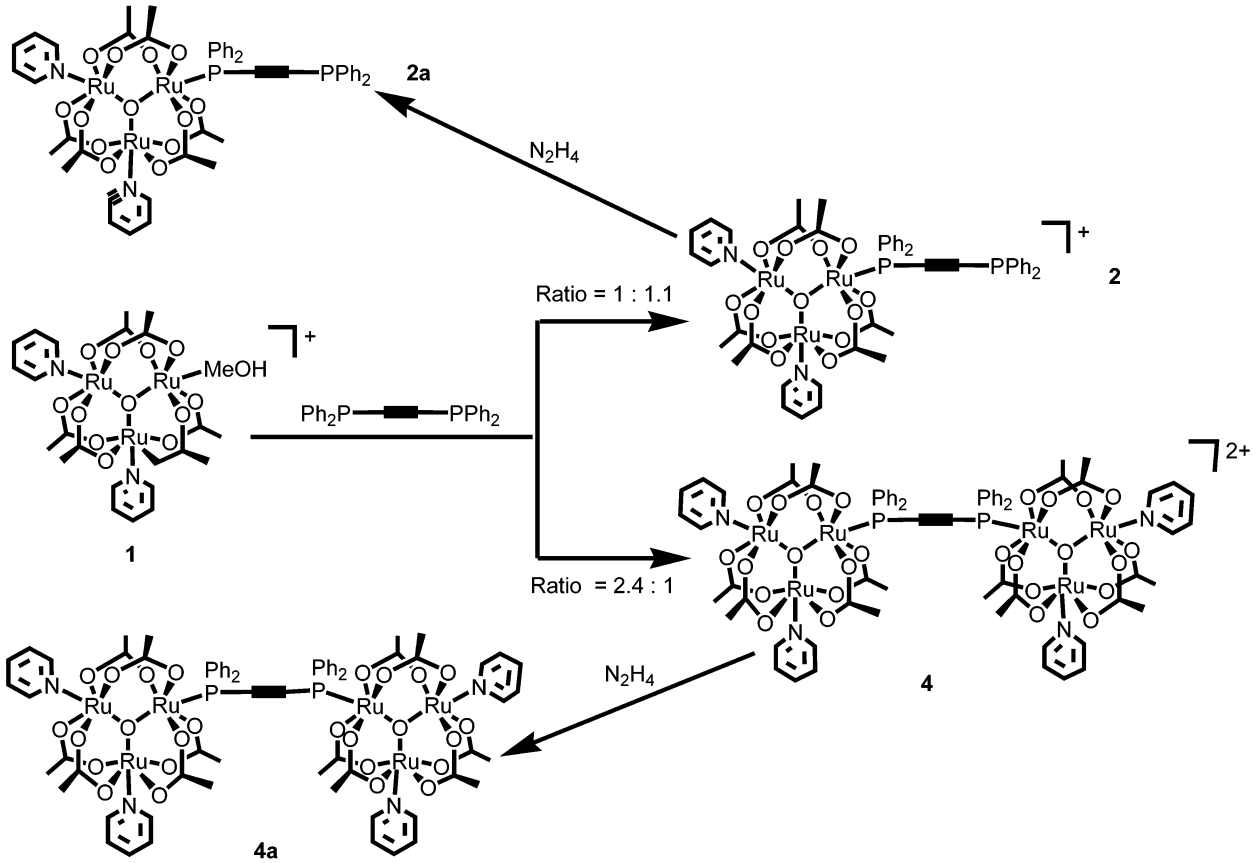

745 (8315), 927 (14 266). ^{31}P NMR spectrum (CD_3CN): δ 24.0 (s, Ru−*P*CH═CHP−Ru).

[{$Ru_3O(OAc)_6(dmap)_2$}$_2$(dppen)](SbF$_6$)$_2$ (6). Complex **1a** (307 mg, 0.259 mmol) and dppen (39.2 mg, 0.099 mmol) were dissolved in dichloromethane (40 mL), and the solution was stirred for 12 h at room temperature. After the volume was reduced to 3 mL, the solution was purified by alumina column chromatography using CH_2Cl_2−CH_3OH (40:1 v/v) as an eluent. The main band (the third fraction) was collected, from which complex **6** was obtained. Yield: 52% (139 mg). Anal. Calcd for $C_{78}H_{98}F_{12}N_8O_{26}P_2Ru_6Sb_2$: C, 34.65; H, 3.65; N, 4.14. Found: C, 34.75; H, 3.68; N, 3.92. ES-MS (*m*/*z*): 1116 $[M - 2SbF_6]^{2+}$, 1315 $[Ru_3O(OAc)_6(dmap)_2(dppen)]^+$, 1193 $[Ru_3O(OAc)_6(dmap)(dppen)]^+$, 950 $[Ru_3O(OAc)_6(dmap)_2(CH_3OH)]^+$. IR spectrum (KBr, cm^{-1}): 1535m (COO), 1415s (COO), 1229m (C−N), 658s (SbF_6). UV−vis spectrum (CH_3CN): λ_{max}/nm (ϵ/dm^3 mol^{-1} cm^{-1}) = 263 (83 270), 424 (24 470), 629 (18 465).

{**[Ru$_3$O(OAC)$_6$(abco)$_2$]$_2$(dppen)**}**(BF$_4$)$_2$ (7).** Complex **1b** (314 mg, 0.31 mmol) and dppen (50.1 mg, 0.126 mmol) were dissolved in dichloromethane (40 mL). After the solution was stirred at room temperature for 12 h, it was evaporated to dryness. The residue was chromatographed on an alumina column using dichloromethane/methanol (50:1 v/v) as the eluent. The main band (the first fraction) was collected, from which complex **7** was obtained. Yield: 50% (150 mg). Anal. Calcd for $C_{78}H_{110}B_2F_8N_4O_{26}P_2Ru_6$: C, 39.67; H, 4.69; N, 2.37. Found: C, 39.56; H, 4.78; N, 2.21. ES-MS (*m*/*z*): 1094 $[M - 2BF_4]^{2+}$, 1293 $[Ru_3O(OAc)_6(abco)_2(dppen)]^+$, 1181 $[Ru_3O(OAc)_6(abco)(dppen)]^+$, 913 $[Ru_3O(OAc)_6(abco)_2(H_2O)]^+$. IR spectrum (KBr, cm^{-1}): 1558m (COO), 1419s (COO), 1057s (BF_4). UV−vis spectrum (CH_2Cl_2): λ_{max}/nm (ϵ/dm^3 mol^{-1} cm^{-1}) = 226 (83 620), 416 (9507), 632 (6100). ^{31}P NMR (CD_3CN): δ 17.6 (s, Ru−*P*CH═CHP−Ru).

Physical Measurements. Elemental analyses (C, H, N) were performed on a Perkin-Elmer Model 240C automatic instrument. The electrospray mass spectra (ES-MS) were recorded on a Finngan LCQ mass spectrometer using dichloromethane−methanol as mobile phase. The UV−vis spectra in acetonitrile solutions were measured on a Perkin-Elmer Lambda 25 UV−vis spectrometer. The IR spectra were recorded on a Magna750 FT-IR spectrophotometer using KBr pellets. The ^{31}P NMR spectra (202.3 MHz) were performed on a Varian UNITY-500 spectrometer with 85% H_3PO_4 as an external standard. The cyclic voltammogram (CV) and differential pulse voltammogram (DPV) were made with a potentiostat/galvanostat Model 263A in acetone solutions containing 0.1 M $(Bu_4N)PF_6$ as supporting electrolyte. CV was performed at a scan rate of 100 mV s^{-1}. DPV was measured at a rate of 20 mV s^{-1} with a pulse height of 40 mV. Platinum and glassy graphite were used as counter and working electrodes, respectively, and the potentials were measured against a Ag/AgCl reference electrode. The potential measured was always referenced to the half-wave potentials of the ferrocenium/ferrocene couple ($E_{1/2}$ = 0.585 V). The procedures for X-ray reflection data collection and crystal structure determination[20] and the crystallographic data (Table S1) were supplied as Supporting Information.

Results and Discussion

Synthesis. The synthetic routes to the series of dppa-attached compounds are shown in Scheme 1. The solvent-coordinated triruthenium clusters $[Ru_3O(OAc)_6L_2(CH_3OH)]^+$ (L = py, **1**; dmap, **1a**; abco, **1b**) were accessible by chemical oxidation of the corresponding carbonyl clusters $Ru_3O(OAc)_6(CO)(L)_2$ using Br_2 (for **1**)[6] or silver salts (for **1a** and **1b**) as oxidants.[19] Attempts to synthesize similar solvent-

coordinated precursor compounds with L = 3-chloropyridine, 4-cyanopyridine, and 4-acetylpyridine were unsuccessful under similar synthetic conditions. Instead, the product isolated appeared to be $[Ru_3O(OAc)_6L_3]^+$. Therefore, triruthenium dimers containing electron-withdrawing substituents on the auxiliary pyridine rings could not be attained in this study.

The weakly coordinated CH_3OH in the precursor compound $[Ru_3O(OAc)_6L_2(CH_3OH)]^+$ can be substituted by rigid diphosphines. Thus, the reaction of $[Ru_3O(OAc)_6L_2(CH_3OH)]^+$ with a nearly equimolar amount of diphosphine (1.1 equiv) gave triruthenium compounds having a monodentate diphosphine (L′) of the type $[Ru_3O(OAc)_6L_2L']^+$. When the molar ratio of $[Ru_3O(OAc)_6L_2(CH_3OH)]^+$ and the diphosphine was employed as 2.4:1, the main product was diphosphine-linked dimer of triruthenium clusters. The product was purified readily by alumina column chromatography. Reduction of the dppa-containing monomeric complexes $[Ru_3O(OAc)_6(py)_2(\eta^1\text{-dppa})](PF_6)$ (**2**) and dppa-linked dimer $[\{Ru_3O(OAc)_6(py)_2\}_2(\mu{:}\eta^2\text{-dppa})](PF_6)_2$ (**4**) using hydrazine gave rise to the isolation of one- and two-electron-reduced neutral compounds $Ru_3O(OAC)_6(py)_2(\eta^1\text{-dppa})$ (**2a**) and $\{Ru_3O(OAC)_6(py)_2\}_2(\mu{:}\eta^2\text{-dppa})$ (**4a**), respectively. A pure sample for the one-electron-reduced product $[\{Ru_3O(OAC)_6(py)_2\}_2(dppa)](PF_6)$ of **4** could not be isolated, probably because of the low comproportionation constant (K_c < 200) (vide infra) in the reaction **4** + **4a**.

In the ^{31}P NMR spectra of dppa-containing triruthenium compound **2**, two singlets were observed at 15.0 and −41.0 ppm, ascribed to the noncoordinated and coordinated P donors of dppa, respectively. As expected, the dppa-linked triruthenium dimer **4** displayed only one singlet at −41.0 ppm assignable to the coordinated P donors of dppa. In both cases, the heptet ($J_{^{31}P-^{19}F}$ = 702−708 Hz) due to the P atom of hexafluorophosphate was observed at −142.5 ppm. Upon reduction to **2a** and **4a**, the heptet disappeared accordingly. The noncoordinated and coordinated P donors of dppa in the one-electron-reduced product **2a** were found as two singlets at 9.1 and −31.5 ppm, respectively. Similar to **4**, only one singlet (−32.2 ppm) was observed for the two-electron-reduced dppa-linked dimer **4a**.

X-ray Crystallography. The structures of **2**, **4**, **5**, **5a**, **6**, and **7** were determined by single-crystal X-ray diffraction. Selected bond distances and angles are summarized in Table 1. ORTEP drawings of the complex cation of **2**, complex cation of **4**, and **5a** are depicted in Figures 1, 2, and 3, respectively.

The Ru_3 skeleton forms approximately isosceles triangle for both monomers and dimers, where one (3.295 (4)−3.323 (4) Å) of the Ru···Ru distances is obviously shorter than the other two (3.380 (5)−3.415 Å). This is ascribable to the trans effect of the diphosphine ligands, making the $Ru-O_{oxo}$ distances (2.012 (9)−2.052 (6) Å) trans to the P donor elongated significantly relative to those of the other two (1.884 (6)−1.912 (9) Å). A similar phenomenon was also observed in the neutral triruthenium and hexaruthenium clusters with axial carbonyl or isocyanides.[5c,d] The sum of the three $Ru-O_{oxo}-Ru$ angles is 360°, and the oxo atom

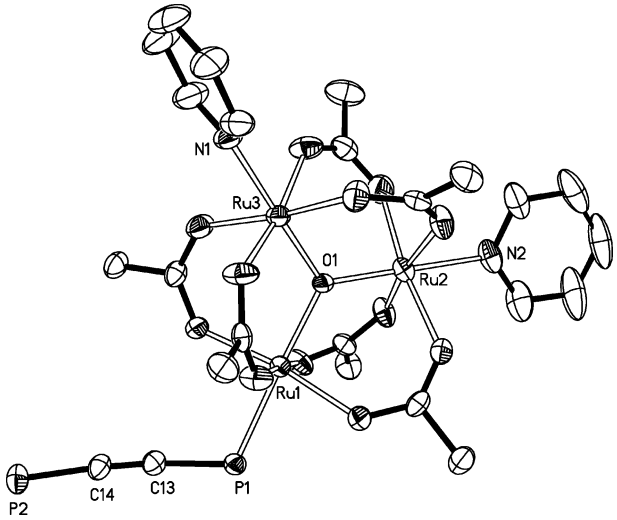

Figure 1. ORTEP drawing of complex cation of **2** (30% thermal ellipsoids) with atom labeling scheme. Phenyl rings on the phosphorus atoms are omitted for clarity.

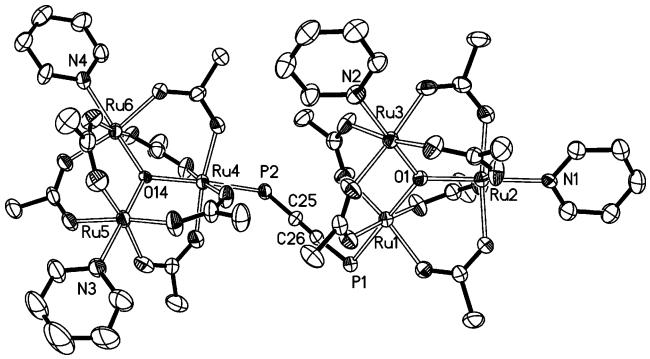

Figure 2. ORTEP drawing of complex cation of **4** (30% thermal ellipsoids) with atom labeling scheme. Phenyl rings on the phosphorus atoms are omitted for clarity.

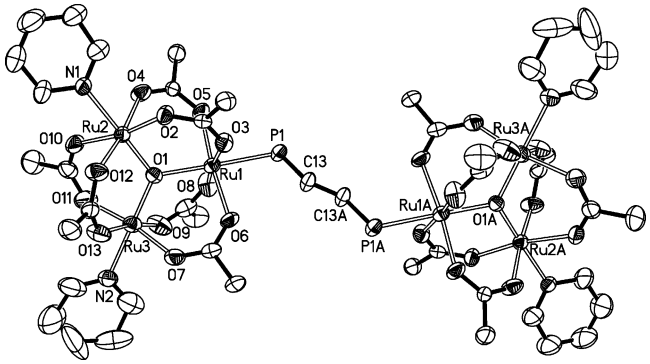

Figure 3. ORTEP drawing of **5a** (30% thermal ellipsoids) with atom labeling scheme. Phenyl rings on the phosphorus atoms are omitted for clarity.

lies approximately in the Ru_3 plane. The intercluster Ru···Ru separations in the dimers of triruthenium clusters through the bridging diphosphines are 6.993, 7.930, 8.009, 7.995, and 8.123 Å for **4**, **5**, **5a**, **6**, and **7**, respectively.

Bonding parameters are compared between dppa-containing monomer (**2**) and dimer (**4**), between dppen-linked dimer (**5**) and its two-electron-reduced species (**5a**), and between dimers **5** and **6** with different axial nitrogen ligands. It is shown that no appreciable variation in atomic distances and bond angles is observed in these comparisons. The bonding

Table 1. Selected Bond Distances [Å] and Angles [deg] for **2**, **4**, **5**, **5a**, **6**, and **7**

	2	**4**	**5**	**5a**	**6**	**7**
Ru···Ru	Ru1···Ru2 3.391(7) Ru1···Ru3 3.383(7) Ru2···Ru3 3.323(8)	Ru1···Ru2 3.392(8) Ru1···Ru3 3.394(7) Ru2···Ru3 3.320(8) Ru4···Ru5 3.395(7) Ru4···Ru6 3.390(6) Ru5···Ru6 3.314(8)	Ru1···Ru2 3.392(7) Ru1···Ru3 3.396(8) Ru2···Ru3 3.295(6)	Ru1···Ru2 3.395(5) Ru1···Ru3 3.380(8) Ru2···Ru3 3.305(7)	Ru1···Ru2 3.397(8) Ru1···Ru3 3.415(6) Ru2···Ru3 3.319(9)	Ru1···Ru2 3.413(4) Ru1···Ru3 3.405(5) Ru2···Ru3 3.315(6)
Ru−O_{oxo}	Ru1−O1 2.016(6) Ru2−O1 1.898(6) Ru3−O1 1.915(6)	Ru1−O1 2.044(7) Ru2−O1 1.904(6) Ru3−O1 1.887(7) Ru4−O14 2.052(6) Ru5−O14 1.887(6) Ru6−O14 1.892(6)	Ru1−O1 2.035(6) Ru2−O1 1.884(6) Ru3−O1 1.902(6)	Ru1−O1 2.033(8) Ru2−O1 1.896(8) Ru3−O1 1.891(7)	Ru1−O1 2.034(9) Ru2−O1 1.907(9) Ru3−O1 1.908(9)	Ru1−O1 2.032(6) Ru2−O1 1.911(6) Ru3−O1 1.906(6)
Ru−N	Ru2−N2 2.130(8) Ru3−N1 2.214(9)	Ru2−N1 2.119(8) Ru3−N2 2.114(9) Ru5−N3 2.013(10) Ru6−N4 2.117(9)	Ru2−N2 2.127(9) Ru3−N1 2.099(9)	Ru2−N1 2.149(11) Ru3−N2 2.131(13)	Ru2−N1 2.116(12) Ru3−N2 2.121(13)	Ru2−N1 2.233(8) Ru3−N2 2.236(8)
Ru−P	Ru1−P1 2.366(3)	Ru1−P1 2.356(3) Ru4−P2 2.354(3)	Ru1−P1 2.351(3)	Ru1−P1 2.365(3)	Ru1−P1 2.372(4)	Ru1−P1 3.374(2)
Ru−O_{oxo}−Ru	Ru1−O1−Ru2 120.0(3) Ru1−O1−Ru3 118.7(3) Ru2−O1−Ru3 121.2(3)	Ru1−O1−Ru2 118.4(3) Ru1−O1−Ru3 119.3(3) Ru2−O1−Ru3 122.2(4) Ru4−O14−Ru5 119.0(3) Ru4−O14−Ru6 118.4(3) Ru5−O14−Ru6 122.6(4)	Ru1−O1−Ru2 119.8(3) Ru1−O1−Ru3 119.2(3) Ru2−O1−Ru3 120.9(3)	Ru1−O1−Ru2 119.5(4) Ru1−O1−Ru3 118.9(4) Ru2−O1−Ru3 121.5(4)		Ru1−O1−Ru2 119.9(3) Ru1−O1−Ru3 119.6(3) Ru2−O1−Ru3 120.50(3)
P−Ru−O_{oxo}	P1−Ru1−O1 177.36(18)	P1−Ru1−O1 178.2(2) P2−Ru4−O14 176.4(2)	P1−Ru1−O1 177.3(2)	P1−Ru1−O1 174.8(2)	P1−Ru1−O1 176.2(3)	P1−Ru1−O1 177.84(18)
Ru−P−C	Ru1−P1−C13 115.3(4)	Ru1−P1−C26 112.0(4) Ru4−P2−C25 110.3(4)	Ru1−P1−C21 109.3(3)	Ru1−P1−C13 108.2(4)	Ru1−P1−C13 109.1(5)	Ru1−P1−C13 113.3(3)

Table 2. Electrochemical Data for Compounds **2**−**7**[a]

compd	$E_{1/2}^{(4+/2+)}$	$E_{1/2}^{(2+/+)}$	$E_{1/2}^{(+/0)}$	$\Delta E'_{1/2}$ (K_c)[c]	$E_{1/2}^{(0/-)}$	$E_{1/2}^{(-/2-)}$	$\Delta E''_{1/2}$ (K_c)[c]
2[b]		+1.270	+0.200		−1.070		
3[b]		+1.250	+0.150		−1.100		
4	+1.280	+0.240	+0.110	0.130 (158)	−1.125	−1.220	0. 095 (40)
5	+1.240	+0.195	+0.090	0.105 (60)	−1.150	−1.235	0.085 (27)
6	+1.100	+0.075	−0.045	0.12 (107)	−1.360	−1.450	0.090 (33)
7	+1.190	+0.100	+0.005	0.095 (40)	−1.370	−1.440	0.070 (15)

[a] Potential data in volts vs Ag/AgCl are from single scan cyclic voltammograms recorded at 25 °C. Detailed experimental conditions are given in the Experimental Section. [b] **2** and **3** are monomers of oxo-centered triruthenium acetate moiety. [c] The comproportionation constants, K_c, were calculated by the formula $K_c = \exp(\Delta E_{1/2}/25.69)$ at 298 K.[21]

parameters are also comparable to the corresponding distances and angles of other oxo-centered triruthenium carboxylate clusters with different axial ligands described in the literature.[15b,c,16c,17] It seems that the rigid molecular skeletons in the triruthenium cluster moieties are insensitive to the variations in both axial and bridging ligands as well as in oxidation number, probably because of the excellent electronic delocalization within the $Ru_3(O)(OAC)_6$ moiety.

In the dppa- and dppen-linked dimers, both the bridging arrays Ru−P−C≡C−P−Ru and Ru−P−CH=CH−P−Ru exhibit zigzag conformations due to sp^3 hybridization of the P donors, where the Ru−P−C angles are in the range 108.2 (4)−115.3 (4)°. The array of Ru−P−CH=CH−P−Ru is coplanar, but that of Ru−P−C≡C−P−Ru is severely twisting. The twist of the array $Ru_3(Ph_2C{\equiv}CPh_2)Ru_3$ in **4** is revealed by the significant dihedral angle of 64.3° between the planes defined by Ru1Ru4P1 and Ru1Ru4P2 (Figure 2), respectively. The two Ru_3 planes are parallel to each other in the dppen-linked triruthenium cluster dimers **5**, **5a**, and **6**, whereas they form a dihedral angle of 75.9° in the dppa-linked dimeric compound **4**.

Redox Properties. The redox properties of compounds **2**−**7** were investigated by cyclic and differential pulse voltammograms. The electrochemical data are presented in Table 2, and the plots of cyclic and differential pulse voltammograms are depicted in Figure 4.

The dppa-attached monomeric triruthenium compound **2** affords three reversible redox processes at $E_{1/2}$ = +1.270, +0.200, and −1.070 V vs Ag/AgCl, corresponding to one-electron couples $[Ru_3^{III,III,IV}]^{2+}/[Ru_3^{III,III,III}]^{+}$, $[Ru_3^{III,III,III}]^{+}/[Ru_3^{II,III,III}]^{0}$, and $[Ru_3^{II,III,III}]^{0}/[Ru_3^{II,II,III}]^{-}$, respectively. The corresponding redox potentials of $[Ru_3O(OAC)_6(py)_3]^{+}$ are +1.091, +0.161, and −0.899 V, respectively, as converted from the data in Ag/Ag^{+}.[15f,16a] It is interesting that the processes $[Ru_3^{III,III,IV}]^{2+}/[Ru_3^{III,III,III}]^{+}$ and $[Ru_3^{III,III,III}]^{+}/[Ru_3^{II,III,III}]^{0}$ in the phosphine complex show more positive potentials relative to those in $[Ru_3O(OAC)_6(py)_3]^{+}$, whereas the reverse trend is observed for the $[Ru_3^{II,III,III}]^{0}/[Ru_3^{II,II,III}]^{-}$ process. The potential gap between $[Ru_3^{III,III,III}]^{+}/[Ru_3^{II,III,III}]^{0}$ and $[Ru_3^{II,III,III}]^{0}/[Ru_3^{II,II,III}]^{-}$ in **2** ($\Delta E_{1/2}$ = 1.27 V) is more pronounced than that in $[Ru_3O(OAC)_6(py)_3]^{+}$ (1.06 V). Consequently, the oxidation state $[Ru_3^{II,III,III}]^{0}$ is more stabilized against disproportionation in the phosphine complex than that in $[Ru_3O(OAC)_6(py)_3]^{+}$. The corresponding potential difference is 1.52 V in the carbonyl complex $[Ru_3O(OAC)_6(py)_2(CO)]$,[15] where strong back-bonding character stabilizes the ruthenium(II) attached by CO against oxidation.

For the dppa-linked dimer **4**, an apparent two-electron-oxidation wave was observed at $E_{1/2}^{(4+/2+)}$ = +1.280 due to the redox couple $[Ru_3^{III,III,IV}{-}dppa{-}Ru_3^{III,III,IV}]^{4+}/[Ru_3^{III,III,III}{-}dppa{-}Ru_3^{III,III,III}]^{2+}$. By contrast, the redox waves involving the $Ru_3^{II,III,III}$ and the $Ru_3^{II,II,III}$ species show obvious splitting. Thus, the $[Ru_3^{III,III,III}]^{+}/[Ru_3^{II,III,III}]^{0}$ process gives two separate redox waves $[Ru_3^{III,III,III}{-}dppa{-}Ru_3^{III,III,III}]^{2+}/[Ru_3^{II,III,III}{-}dppa{-}Ru_3^{III,III,III}]^{+}$ and $[Ru_3^{II,III,III}{-}dppa{-}Ru_3^{III,III,III}]^{+}/[Ru_3^{II,III,III}{-}dppa{-}Ru_3^{II,III,III}]^{0}$ at +0.240 and +0.110 V, respectively. The extent of the splitting is $\Delta E'_{1/2}$ = 0.130 V, which corresponds to a comproportionation constant K_c (=$[(Ru_3^{II,III,III}{-}dppa{-}Ru_3^{III,III,III})^{+}]^2/[(Ru_3^{III,III,III}{-}dppa{-}Ru_3^{III,III,III})^{2+}][(Ru_3^{II,III,III}{-}dppa{-}Ru_3^{II,III,III})^{0}]$) = 158. The splitting of the second redox wave is $\Delta E''_{1/2}$ = 0.095 V, which corresponds to K_c = 40, where the redox processes $[Ru_2Ru^{III,III,II}{-}dppa{-}Ru_2Ru^{III,III,II}]^{0}/[RuRu_2^{III,II,II}{-}dppa{-}Ru_2Ru^{III,III,II}]^{-}$ and $[RuRu_2^{III,II,II}{-}dppa{-}Ru_2Ru^{III,III,II}]^{-}/[RuRu_2^{III,II,II}{-}dppa{-}RuRu_2^{III,II,II}]^{2-}$ are observed at $E_{1/2}^{(0/-)}$ = −1.125 and $E_{1/2}^{(-/2-)}$ = −1.220 V, respectively.

It is interesting that even the π conjugation is blocked by the sp^3 P donors; the diphosphine ligand can still mediate the redox interactions between the two triruthenium centers. This may be due to some π-back-bonding character of the phosphine ligand as evidenced by the stabilization of $Ru_3^{II,III,III}$ state (vide supra). The degree of electronic communication between two triruthenium moieties through bridging dppa is less efficient compared with that across bridging pyrazine,[5a,b,6a,c] but close to that through 1,4-phenylene diisocyanide.[5c] It is interesting to notice that the potential separation ($\Delta E_{1/2}$) between the oxidation processes $E_{1/2}^{(2+/+)}$ and $E_{1/2}^{(+/0)}$ ($\Delta E'_{1/2}$ = 0.130 V) is more pronounced than that between the reduction processes $E_{1/2}^{(0/-)}$ and $E_{1/2}^{(-/2-)}$ ($\Delta E''_{1/2}$ = 0.095 V). A similar situation occurs in the 1,4-phenylene diisocyanide bridged neutral dimers $[\{Ru_3(O)(OAC)_6(L)_2\}_2(CNC_6H_4NC)]$ (L = py, dmap),[5c] but it presents a striking contrast to the general observation for the magnitude of redox wave splitting in pyrazine-bridged triruthenium dimers which exhibit a reverse trend.[5a,b,6a,c] In the pyrazine-bridged dimer $[\{Ru_3O(OAC)_6(py)_2\}_2(pyz)]^{2+}$ (pyz = pyrazine),[6a,c] the wave splitting between the oxidation processes $E_{1/2}^{(2+/+)}$ and $E_{1/2}^{(+/0)}$ ($\Delta E'_{1/2}$ = 0.10 V) is significantly smaller than that between the reduction processes $E_{1/2}^{(0/-)}$ and $E_{1/2}^{(-/2-)}$ ($\Delta E''_{1/2}$ = 0.27 V). For the pyrazine-bridged dimer $[\{Ru_3O(OAC)_6(py)(CO)\}_2(pyz)]$,[5a,b] while the wave splitting was unobserved between the couples $E_{1/2}^{(2+/+)}$ and $E_{1/2}^{(+/0)}$, a remarkable wave separation is present between the redox couples $E_{1/2}^{(0/-)}$ and $E_{1/2}^{(-/2-)}$ with $\Delta E_{1/2}$

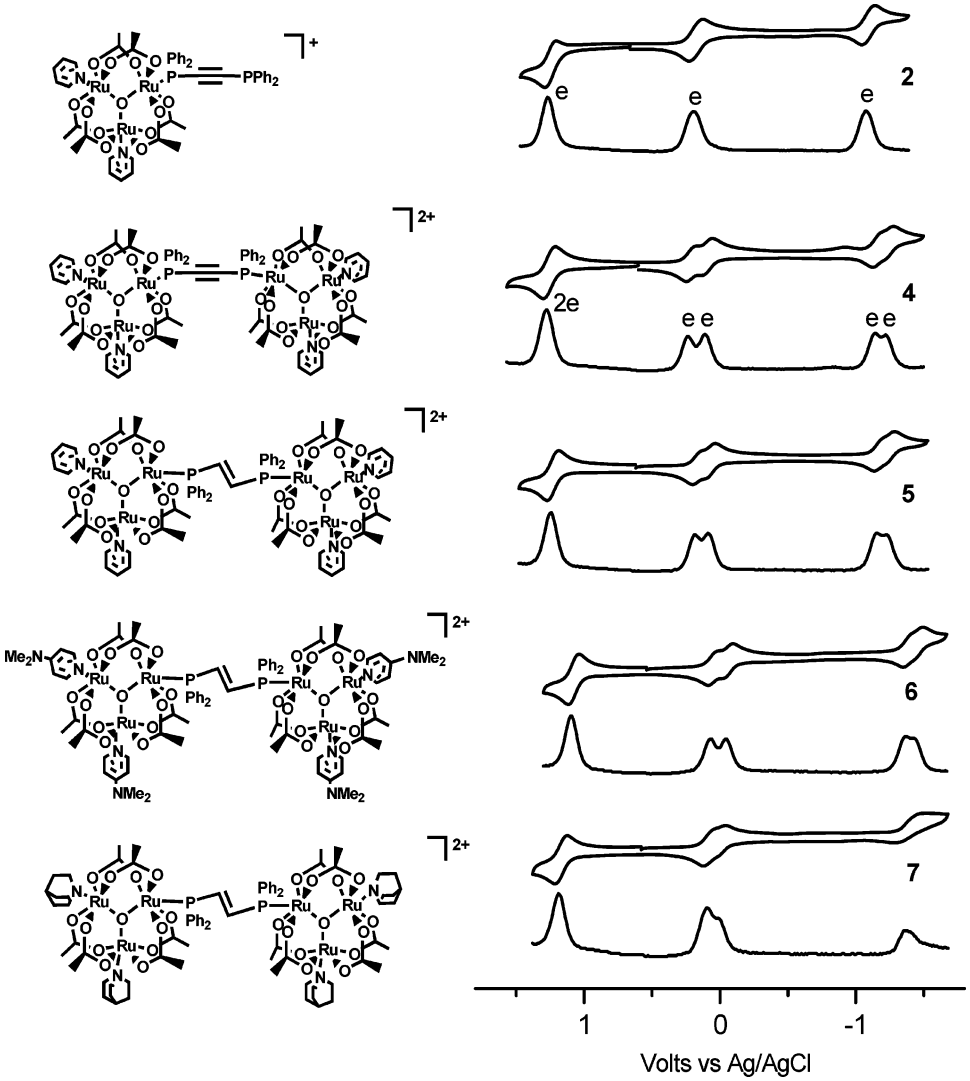

Figure 4. Molecular drawings (left) and cyclic and differential pulse voltammograms (right) of diphosphine-containing monomers **2** and dimers **4**−**7** of oxo-centered triruthenium acetate cluster moieties recorded in 0.1 M acetone solution of $(Bu_4N)(PF_6)$. The scan rate is 100 mV s^{-1} for CV and 20 mV s^{-1} for DPV.

as high as 0.38 V. In 1,4-phenylene diisocyanide bridged neutral dimers $[\{Ru_3(O)(OAC)_6(L)_2\}_2(CNC_6H_4NC)]$ (L = py, dmap),[5c] it has been suggested that the electron introduced by the reduction in the process $[Ru_2Ru^{III,III,III}-CNC_6H_4NC-Ru_2Ru^{III,III,III}]^{2+}/[RuRu_2^{III,III,II}-CNC_6H_4NC-RuRu_2^{III,III,II}]^0$ would be localized at the bridging Ru site almost completely due to the electron-withdrawing character of the bridging CNC_6H_4-NC ligand, whereas the process $[Ru_2Ru^{III,III,II}-CNC_6H_4NC-Ru_2Ru^{III,III,II}]^0/[RuRu_2^{III,II,II}-CNC_6H_4NC-RuRu_2^{III,II,II}]^{2-}$ shows no redox wave splitting, suggesting that reduction occurs at the nonbridging Ru sites. With this suggestion, it is likely that the redox, associated with the process $[Ru_2Ru^{III,III,III}-dppa-Ru_2Ru^{III,III,III}]^{2+}/[RuRu_2^{III,III,II}-dppa-RuRu_2^{III,III,II}]^0$ which shows a larger wave splitting, would be localized mainly at the bridging Ru site, whereas the reduction, associated with the process $[Ru_2Ru^{III,III,II}-dppa-Ru_2Ru^{III,III,II}]^0/[RuRu_2^{III,II,II}-dppa-RuRu_2^{III,II,II}]^{2-}$ with a smaller wave splitting, would mainly occur at the nonbridging Ru sites.

The magnitude of redox interaction can be modulated by modification of the bridging spacers. By comparison of the electrochemical data for **4** and **5**, it is observed, whether wave splitting $\Delta E'_{1/2}$ between the oxidation processes $E_{1/2}^{(2+/+)}$ and $E_{1/2}^{(+/0)}$ or $\Delta E''_{1/2}$ between the reduction processes $E_{1/2}^{(0/-)}$ and $E_{1/2}^{(-/2-)}$, that the corresponding values in **4** ($\Delta E'_{1/2}$ = 0.130 V, $\Delta E''_{1/2}$ = 0.095 V) are obviously higher than those in **5** ($\Delta E'_{1/2}$ = 0.105 V, $\Delta E''_{1/2}$ = 0.085 V). This is evidence to show that ethynyl-linked diphosphine (dppa) is better at transmitting the electronic effect than dppen with ethenyl spacer between two P donors. A direct explanation for this phenomenon is the shorter intramolecular $Ru_3\cdots Ru_3$ distance through the bridging dppa (ca. 7.0 Å) than that through dppen (ca. 8.0 Å).

The redox wave splitting between two triruthenium redox centers can also be tuned by changing the ancillary ligands, which are bonded axially. Comparing dppen-bridged dimers **5** and **6**, it is observed that through substitution of the axially coordinated pyridine with *N*,*N*-(dimethylamino)pyridine the wave splitting in **6** ($\Delta E'_{1/2}$ = 0.120 V, $\Delta E''_{1/2}$ = 0.090 V) becomes more pronounced relative to that in **5** ($\Delta E'_{1/2}$ = 0.105 V, $\Delta E''_{1/2}$ = 0.085 V). A similar phenomenon was

also revealed in the pyrazine-bridged dimers of carbonyl-containing triruthenium moiety,[5a,b] where the axially bonded pyridines with electron-donating substituent afforded stronger electronic communication than that with electron-withdrawing substituent. Nevertheless, the potential separations $\Delta E'_{1/2}$ and $\Delta E''_{1/2}$ in the dppen-bridged dimer **7** with an axial ligand abco ($\Delta E'_{1/2} = 0.105$ V, $\Delta E''_{1/2} = 0.085$ V) are smaller than those in **5** with pyridine as an ancillary ligand ($\Delta E'_{1/2} = 0.095$ V, $\Delta E''_{1/2} = 0.070$ V). This is in contrast with that found in the neutral pyrazine-bridged dimer of carbonyl-attached triruthenium moiety,[5d] in which abco as the ancillary ligand is more favorable than pyridine for the electronic communication.

The origin of redox wave splitting for the ligand-bridged dimers of triruthenium moieties mainly results from two contributions. One is ligand-mediated electronic delocalization between Ru_3 clusters. An orbital pathway for electronic interaction between clusters exists on the basis of the π or π^* systems of the bridging ligands.[6] It has been suggested that electronic delocalization between clusters is an important feature in the mixed-valence dimer $[\{Ru_3O(OAC)_6(py)_2\}_2(pyz)]^+$ and even more so in the dimer $[\{Ru_3O(OAC)_6(py)_2\}_2(pyz)]^-$ (pyz = pyrazine).[6a,c] Based on the molecular orbital diagram for the $Ru_3(O)$ core proposed by Meyer,[6a] cluster−cluster electronic interactions are expected to be the greatest for the −1 mixed-valence ion since the additional electron is added to the Ru−O−Ru antibonding orbital. Taking into account the stronger π character of pyrazine relative to that of diphosphine, it is easy to understand the weaker electronic delocalization between Ru_3 clusters across bridging diphosphine. The less π character of phosphine causes less contribution of the bridging Ru atom to the molecular orbital in the diphsphine complexes. The other origin of redox wave splitting is possibly from electrostatic effect mediated through space.[6] In view of the weak π character in phosphine ligand, it is likely that the electrostatic effect through space is an important origin for the wave splitting in the diphosphine-bridged dimers of triruthenium moieties.

The magnitude of potential separation ($\Delta E_{1/2}$) due to wave splitting is determined by two main factors. One is the distance between the redox centers. The shorter the distance, the stronger the electronic communication, if the degree of π conjugation is the same. The appreciably larger $\Delta E_{1/2}$ in the dppa-bridged dimer **4** relative to that in the dppen-bridged dimer **5** is the result of the shorter intercluster distance in the former than in the latter. The other factor that determines the potential separation is an energy match between the π molecular orbital of the Ru_3 cluster and the bridging ligand π^* orbital through which electronic interaction is operative.[5c,6a] Unoptimizable match of energy levels between the Ru_3 cluster π orbital and the diphosphine π^* orbital is likely another important factor for the small $\Delta E_{1/2}$ in the diphosphine-bridged dimers. When the axially coordinated ligand py is changed into dmap, the Ru_3 cluster π orbital level becomes closer to the diphosphine π^* orbital level, and thus leads to a larger $\Delta E_{1/2}$. Nevertheless, when abco serves as the axial ligand instead of py, the energy difference between the Ru_3 cluster π orbital level and the diphosphine π^* orbital level increases, thus resulting in a smaller $\Delta E_{1/2}$.

UV−vis Spectra. The electronic absorption spectra show three absorption bands at 232, 404, and 648 nm in the triruthenium complex **2** (Figure S1) containing dppa ligand. The high-energy band is due to a $\pi-\pi^*$ transition of the ligand, whereas the two low-energy bands can be assigned to a cluster-to-ligand charge-transfer transition (CLCT).[5,6] The absorption spectra of dppa-bridged dimer **4** (Figure S2) show an inappreciable change or shift compared with those of **2**. The one-electron-reduced product **2a**, however, displays quite different absorption spectra from **2**. Besides the bands due to $\pi-\pi^*$ transition of the ligand and cluster-to-ligand charge-transfer transition, a broad near-IR absorption band centered at 907 nm was observed which is likely derived from the electronic delocalization within $Ru_3^{II,III,III}$ cluster.[5] Compared with one-electron-reduced $Ru_3^{II,III,III}$ complex **2a**, two-electron-reduced $Ru_3^{II,III,III}$−dppa−$Ru_3^{II,III,III}$ product **4a** shows almost the same absorption bands. For the intercluster mixed-valence intermediate compound $[Ru_3^{II,III,III}$−dppa−$Ru_3^{III,III,III}]^+$ generated by mixing an equimolar amount of **4** $[Ru_3^{III,III,III}$−dppa−$Ru_3^{III,III,III}]^{2+}$ and **4a** $[Ru_3^{II,III,III}$−dppa−$Ru_3^{II,III,III}]^0$, the most interesting spectral feature is an absorption band due to intercluster intervalence charge transfer (IVCT). This band, however, is unobserved due to probably the considerable low extinction coefficient of this band which is covered severely by the CLCT or Ru_3 cluster-centered charge-transfer bands.

Conclusion

A series of oxo-centered triruthenium acetate cluster monomers and dimers with ethynyl-/ethenyl-linked diphosphine spacers have been prepared and characterized structurally. The one- or two-electron-reduced tri- and hexanuclear ruthenium complexes with mixed valences have also been accessed by chemical reduction reactions. It is demonstrated that electronic communication is operative between oxo-centered triruthenium moieties mediated by rigid conjugated diphsophine. Furthermore, the wave splitting between the oxidation processes $E_{1/2}^{(2+/+)}$ and $E_{1/2}^{(+/0)}$ is more pronounced than that between the reduction processes $E_{1/2}^{(0/-)}$ and $E_{1/2}^{(-/2-)}$, which is in contrast with that observed previously in the pyrazine-bridged dimers of triruthenium moieties. It has been observed that the wave splitting between two triruthenium moieties across bis(diphenylphosphino)acetylene (dppa) is more remarkable than that across *trans*-1,2-bis(diphenylphosphino)ethylene (dppen). It has also been shown that substitution of the axially coordinated pyridine with *N*,*N*-(dimethylamino)pyridine leads to more pronounced electronic communication between two redox centers of triruthenium moieties.

Acknowledgment. This work was supported financially by NSF of China, NSF of Fujian Province, the fund of the Chinese Academy of Sciences, and the national basic research program (001CB1089) from the Ministry of Sciences and Technology of China.

Supporting Information Available: Detailed procedures for reflection data collection and structural determination: crystal-

lographic data (Table S1); electronic absorption spectra of **2** and **2a** (Figure S1) and **4** and **4a** (Figure S2) in acetonitrile, and X-ray crystallographic files in CIF format for the structural determinations of compounds **2**, **4**·$C_2H_4Cl_2$, **5**·$2CH_2Cl_23H_2O$, **5a**·$CH_2Cl_24H_2O$, **6**·$MeOH·(5/2)H_2O$, and **7**·$8H_2O$. This material is available free of charge via the Internet at http://pubs.asc.org.

IC0344968